

Soft X-ray and ultraviolet observations of Mrk 841: implications for the blue bump

K. Nandra,¹ T. J. Turner,^{2,3} I. M. George,^{2,3} A. C. Fabian,¹ C. Shrader^{4,3} and W.-H. Sun⁵

¹*Institute of Astronomy, Madingley Road, Cambridge CB3 0HA*

²*Laboratory for High Energy Astrophysics, Code 668, NASA/Goddard Space Flight Center, Greenbelt, Maryland, MD 20771, USA*

³*Universities Space Research Association*

⁴*CGRO Science Support Center, Code 668.1, NASA/Goddard Space Flight Center, Greenbelt, MD 20771, USA*

⁵*Institute of Astronomy and Department of Physics, National Central University, Chung-Li, Taiwan 32054, Republic of China*

Accepted 1994 September 29. Received 1994 June 9; in original form 1994 April 21

ABSTRACT

We present an analysis of an extended *ROSAT* observation of the Seyfert galaxy Mrk 841. The source is clearly variable on short time-scales with distinctive changes in the hardness ratio, indicating that more than one spectral component is present in the PSPC band. Spectral modelling of the soft X-ray data confirms this complex picture. The data show that the continuum is particularly steep in the soft band ($\Gamma = 2.4$). We find that the soft X-ray spectrum is best fitted by models in which the primary power law is modified either by absorption by highly ionized material in the line of sight, or by an additional emission component which contributes to the lowest PSPC channels. Simultaneous spectral fitting of the PSPC data and the UV continuum data, which were obtained contemporaneously with *IUE*, show that the best-fitting power law in the soft X-ray extrapolates well into the UV and carries the bulk of the source power. We have been unable to find a satisfactory fit to the UV/soft X-ray emission with standard accretion disc models. One possibility is that the disc spectrum is modified substantially by Comptonization in a corona above the disc. Future variability data should allow us to test this model.

Key words: galaxies: active – galaxies: individual: Mrk 841 – galaxies: nuclei – galaxies: Seyfert – X-rays: galaxies.

1 INTRODUCTION

Multiwavelength observations of radio-quiet active galactic nuclei (AGN) have suggested that the peak of emission occurs in the UV/soft X-ray region of the spectrum, the so-called ‘blue bump’ (Shields 1978; Malkan & Sargent 1982). If the emission in AGN is powered by accretion on to a supermassive black hole (e.g. Rees 1984), as seems most likely, the blue bump may be identified with thermal emission from the accreting material. As the material is likely to possess some angular momentum, an accretion disc seems the most likely geometry. An alternative picture was proposed by Guilbert & Rees (1988), who suggested that the blue bump may not arise from *intrinsic* emission, but simply consist of ionizing radiation which has been reprocessed by optically thick material close to the central source. Support for the existence of near-neutral optically thick gas, including

an accretion disc, close to the continuum source in AGN has been provided by the *Ginga* satellite. Features due to absorption, fluorescence and Compton scattering in the gas are imprinted on the X-ray spectrum, and can be detected at X-ray wavelengths (e.g. Nandra & Pounds 1994, and references therein). Although it is difficult to distinguish between the possible geometries using the X-ray data alone, the mean parameters for Seyfert galaxies observed by *Ginga* are in remarkable agreement with those expected from a disc. One of the implications of the X-ray observations is that substantial reprocessing of the X-ray photons should occur, even for an accretion disc. Indeed, the rapid, colour-independent variations of the Seyfert galaxy NGC 5548 can only be reconciled with disc models if the bulk (perhaps all) of the optical and ultraviolet continuum flux arises via reprocessing in the disc (Clavel et al. 1991, 1992). However, while the blue bump emission is predicted from accretion

disc and reprocessing models, and the turn-up in the UV and soft X-ray excesses imply a peak at the right energy, few high-quality simultaneous UV/X-ray spectral data have been presented thus far. Observations with the *ROSAT* PSPC have offered unprecedented resolution and sensitivity in the soft X-ray (0.1–2.0 keV) band, and provide an ideal opportunity to study the shape of the XUV emission.

Mrk 841 (PG 1501+106; $z=0.036$) is a radio-quiet, Seyfert 1-type active galaxy. It is one of the archetypal ultraviolet-excess objects and was the first Seyfert to show a distinctive soft X-ray excess, based on *EXOSAT* data (Arnaud et al. 1985). This excess has been interpreted as the high-energy tail of the blue bump emission described above. A detailed analysis of later X-ray data obtained for Mrk 841 was presented by George et al. (1993, hereafter G93). The soft excess was confirmed and, at harder energies, G93 found the source to exhibit an iron line and hard tail. The Fe $K\alpha$ line in this source was found to be unusually strong, implying a reflection component substantially greater than that expected from an accretion disc, the most likely source of the spectral features seen in the bulk of *Ginga* Seyferts (e.g. Lightman & White 1988; George & Fabian 1991). In addition, substantial changes in the spectral shape were observed, with dramatic changes in the apparent power-law spectral index ($\Delta\Gamma \sim 0.6$). These were also interpreted in the context of the reflection model, as changes in the relative contributions of direct and reflected continua. G93 found no evidence for an intrinsic cold column density $N_{\text{H}} \geq \text{few} \times 10^{20} \text{ cm}^{-2}$. Pounds et al. (1994) have presented simultaneous *Ginga* and *ROSAT* observations of Mrk 841 and obtain similar results to G93. They find an adequate fit to the combined data set with a reflection model and additional soft component, although an acceptable fit can be obtained without the soft excess, if partially ionized gas exists in the line of sight.

Here we present results from an extended ~ 20 -ks *ROSAT* observation of Mrk 841, together with contemporaneous *IUE* observations. The soft excess first discovered by Arnaud et al. (1985) is confirmed, and the greater spectral resolution of the PSPC has given us better constraints on the spectral shape. We have used the soft X-ray and UV data obtained for Mrk 841 to constrain models for the continuum emission in the UV/soft X-ray regime.

2 OBSERVATIONS

2.1 X-ray

The X-ray data described here were derived from two separate observations made in 1992 January using the X-ray telescope (XRT) on board the *ROSAT Observatory* (Trümper 1983) with the position sensitive proportional counter (PSPC; Pfeffermann et al. 1987). The first, longer observation began on 1992 January 20 at 04^h02^m51^s (UTC) and was performed over ~ 6 d, with an on-source exposure time of 17 185 s. The second observation started on 1992 January 21 at 05^h38^m50^s (UTC) and had an exposure time of 2961 s. The data from the second observation therefore served to ‘fill in’ a large gap in the longer exposure.

The data for each observation were analysed using the Starlink ASTERIX system. After examination of the image, spectra and time series were extracted from a circular source cell with a radius of 3 arcmin, sufficient to collect all the source photons for an on-axis observation given the width of the PSPC point-spread function (Hasinger et al. 1992). The background was estimated from an adjacent source-free region. The count rates were corrected for dead-time.

For the spectral analysis described below, we extracted a 256-channel, pulse-invariant (PI) spectrum. We ignored PI channels 1–11 and those above 250, and rebinned the remaining channels into 32 bins. We have added systematic errors amounting to 2 per cent of the count rate to the statistical error in each resultant bin, to account for residual uncertainties in the spectral calibration of the detector. The spectral analysis was performed using the PSPC response matrix released on 1993 January 12. The mean count rate in the 0.1–2.0 keV band was found to be $2.14 \pm 0.02 \text{ count s}^{-1}$, corresponding to an observed flux of $1.78 \times 10^{-11} \text{ erg cm}^{-2} \text{ s}^{-1}$, assuming the best-fitting power law and Galactic N_{H} described below (Table 1, line 2). The inferred unabsorbed flux was $3.7 \times 10^{-11} \text{ erg cm}^{-2} \text{ s}^{-1}$ in this same band.

2.2 Ultraviolet

Ultraviolet spectroscopic observations of Mrk 841 were made on 1992 January 18.7, using the short- and long-wavelength prime (SWP and LWP) cameras on-board the *International Ultraviolet Explorer* (*IUE*, Sonneborn et al.

Table 1. Fits to the Mrk 841 PSPC spectrum. The models are A power law; B power law plus blackbody; and C power law plus warm absorber.

Model	A_{pl}^a	Γ	A_{bb}^b	kT	N_{H}	$\log N_{\text{H}}^*$	$\log U^c$	$\chi^2_{\nu}/\text{d.o.f.}$
	10^{-3}		10^{-3}	(eV)	(10^{20} cm^{-2})	cm^{-2}		
A.	5.25	$2.39^{+0.05}_{-0.04}$	–	–	2.14 ± 0.11	–	–	1.45/29
A.	5.32	$2.42^{+0.01}_{-0.01}$	–	–	2.2 (F)	–	–	1.42/30
B.	5.01	$2.17^{+0.09}_{-0.11}$	0.09 ± 0.03	75^{+5}_{-5}	2.2 (F)	–	–	0.59/28
C.	6.13	$2.40^{+0.02}_{-0.04}$	–	–	2.2 (F)	$21.37^{+0.24}_{-0.28}$	$-0.24^{+0.18}_{-0.14}$	0.69/28

^aPower-law normalization (flux at 1 keV) in units of $10^{-3} \text{ photon cm}^{-2} \text{ s}^{-1} \text{ keV}^{-1}$.

^bBlackbody normalization.

^cIonization parameter, $U = Q/4\pi n_{\text{H}} r^2 c$ (see text).

1987). Both spectra were well centred in the aperture. Typical UV continuum flux levels for Mrk 841 are a few $\times 10^{-14}$ erg cm $^{-2}$ s $^{-1}$ Å $^{-1}$. In this case, our 200-min SWP observation (SWP 43679) resulted in a well-exposed image, whereas the 100-min LWP spectrum (LWP 22271) appeared underexposed.

Initial processing of the data was performed by the NASA/GSFC staff using the standard IUESIPS software (e.g. Harris & Sonneborn 1987). We then used the software at the GSFC Regional Data Analysis Facility to apply a Gaussian-weighted extraction slit to the ‘line-by-line’ images, resulting in flux- and wavelength-calibrated spectra. In addition to this Gaussian extraction process, spectra obtained by the standard IUESIPS extraction procedure were analysed for comparison. No gross differences in the continuum flux levels were discernible.

Upon examining the spectra, it became apparent that a discontinuity existed in the continuum energy distribution between the SWP and LWP portions of the composite *IUE* spectrum. The SWP flux levels were consistent with a number of archival *IUE* spectra for Mrk 841, whereas the LWP continuum flux seemed anomalously low. The only other concurrently obtained pair of SWP–LWP spectra available from the NSSDC *IUE* archive were examined and found to exhibit no such continuum discontinuity. Through discussions with the observatory staff, we learned of several other cases of anomalous LWP ‘underexposures’ in 1991/92. No such behaviour has been reported for the SWP. We thus concluded that our LWP image was affected either by a data-processing or on-board instrument anomaly during our exposure, and that the SWP data are accurate to within the nominal 10 per cent absolute calibration uncertainty. For subsequent analysis in this paper we will therefore use only the SWP portion of the spectrum.

We estimated the true continuum value at regions free from obvious line features using bins of 80–100 Å. The standard deviation of the point in each bin was used to determine the uncertainty. As our LWP spectrum was corrupted, we have used an archival data set (SWP 19213 and LWP 15200, obtained in 1983 February) to examine the 2200-Å decrement, which in any case is very small. From this, we estimate a Galactic reddening of $E(B-V) \leq 0.02$. Such a value is consistent with the small Galactic column density towards Mrk 841 derived from 21-cm measurements ($N_H = 2.2 \times 10^{20}$ cm $^{-2}$; Elvis, Lockman & Wilkes 1989) and X-ray observations (G93). Since such a reddening will only give a change in the spectra index of ≤ 0.05 in the SWP (negligible when compared to the statistical errors), no correction for reddening has been applied to the data reported here.

3 X-RAY RESULTS

3.1 Temporal analysis

The X-ray light curve, binned \sim once per *ROSAT* orbit, is shown in Fig. 1. It can be seen that the count rate in the total (0.1–2.5 keV) PSPC band (top panel) varies by ~ 50 per cent during the course of the observation. Examining the count rates in the hard (1.0–2.5 keV) and soft (0.1–0.4 keV) bands separately, it is clear that, whilst characteristics of the variability are broadly similar (middle panels), the soft flux

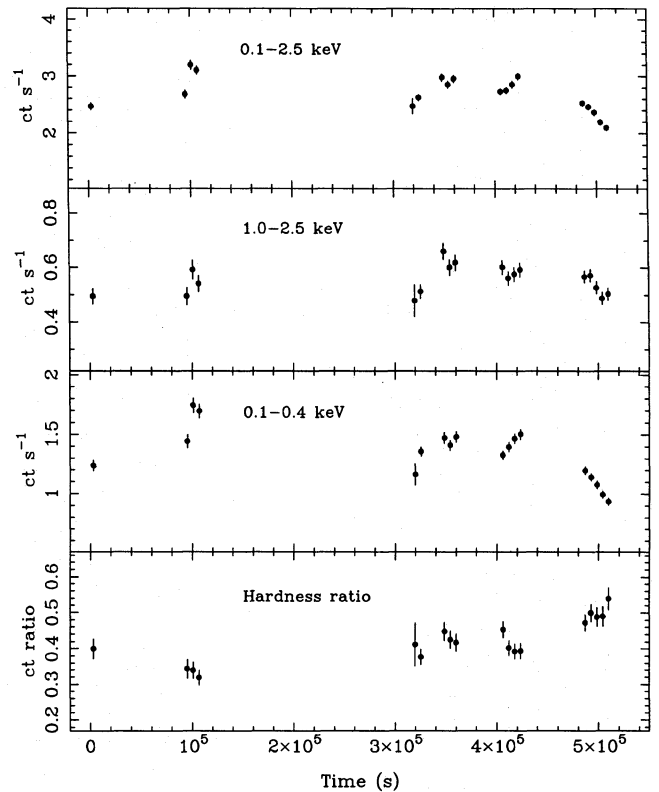


Figure 1. Variations in the observed PSPC count rates as a function of time. The top panel shows the time series for the full PSPC energy-band. Clear variations are present in the source flux, by a factor ~ 50 per cent. Interestingly, however, these flux changes are not colour-independent, as can be seen by the light curves in hard and soft bands (middle panels). Whilst the variability is broadly correlated in both bands it is not identical, a fact which is further illustrated by the hardness ratio (bottom panel).

varies by a larger factor than the hard. This is further demonstrated by the hardness ratio (bottom panel), which shows variations both on short time-scales (i.e., between orbits), and as part of a longer (\sim daily) trend. Thus it is clear that Mrk 841 exhibited significant spectral variability during the observations. This suggests that there may be two spectral components in the PSPC band, which vary independently. However, as we shall see below, the current data do not allow us to distinguish between additional emission or absorption components, or even a single component with variable spectral shape.

3.2 Spectral analysis

We consider here only the mean spectrum summed over the entire observing period rather than the spectra of individual orbits, as the signal-to-noise ratio for these short data sets is insufficient to produce meaningful results. Using this method we can characterize the time-averaged properties, which in any case is necessary when comparing the X-ray data to those obtained contemporaneously in the UV (Section 3). We have compared this mean spectrum to various trial models. Throughout this work, errors are quoted at 68 per

cent confidence for all but one parameter treated as interesting.

From Table 1 it can be seen that a simple power-law model (described by a photon flux $F(E) = A_{\text{pl}} E^{-\Gamma} \exp(-\sigma_{\text{ph}} N_{\text{H}})$; σ_{ph} is the photoelectric absorption cross-section given by Morrison & McCammon 1983), with N_{H} free (line 1) or fixed at the Galactic column density $N_{\text{H}} = 2.2 \times 10^{20} \text{ cm}^{-2}$ (Elvis et al. 1989, line 2), was only marginally acceptable (with reduced chi-squared $\chi^2_{\nu} = 1.45$ and 1.42, respectively) and can be rejected with ~ 95 per cent confidence. However, these fits confirm the claim of G93 that there is no significant cold N_{H} intrinsic to Mrk 841 and show a soft X-ray cut-off entirely compatible with absorption by H I in our Galaxy. We have therefore fixed the column at the H I value in all subsequent fits.

Arnaud et al. (1985) first modelled the excess in the observed soft X-ray flux (over that predicted by extrapolation of the hard X-ray spectrum) as a low-temperature blackbody component. This model has since become a useful parametrization of AGN soft X-ray spectra, and so we applied it to Mrk 841 for comparison with previous results. The results from fitting this model to these data are shown in Table 1 (line 3). It can be seen that a temperature of 75 eV provides an acceptable fit ($\chi^2_{\nu} = 0.59$) with an underlying photon index of $\Gamma \approx 2.2$. The best-fitting count spectrum and data-minus-model residuals are shown in Fig. 2(a).

Recent high signal-to-noise PSPC observations have revealed strong evidence for ionized oxygen VII/VIII absorption edges in several Seyfert galaxies (Nandra & Pounds 1992; Fiore et al. 1993; Nandra et al. 1993; Turner,

George & Mushotzky 1993; Turner et al. 1993). Such a feature is a signature of highly ionized gas (the so-called warm absorber) along the line of sight to the continuum source. It seems highly plausible that such gas could be present in Mrk 841 – indeed, Pounds et al. (1994) found that an acceptable fit could be obtained to the entire 0.1–20 keV spectrum of Mrk 841 with a power-law, warm absorber and reflection spectrum. We have therefore tested our spectrum for the presence of ionized gas. We have used the warm absorber model of Yaqoob & Warwick (1991), which assumes solar abundances and neglects X-ray emission lines. From the results given in Table 1 (line 4), it can be seen that a model comprised of an underlying power law plus a warm absorber gives an excellent fit to the data ($\chi^2_{\nu} = 0.69$). Our best-fitting results in an ionized hydrogen column density $N_{\text{H}}^* = 2.3 \times 10^{21} \text{ cm}^{-2}$ and an ionization parameter of $U = 0.58$, where U is defined as $U = Q/4\pi n_{\text{H}} r^2 c$. Here Q is the flux of ionizing photons, n_{H} the gas density, and r is the distance of the absorbing medium from the ionizing source. The best-fitting count spectrum and data-minus-model residuals are shown in Fig. 2(b).

Finally, recent soft X-ray observations of a number of Seyfert galaxies have revealed evidence for emission lines in the 0.6–1.0 keV band (Turner et al. 1991; Turner, George & Mushotzky 1993). Although we find no evidence for an emission line in our spectrum, we have applied such a model to the PSPC data reported here. An additional Gaussian component with energy fixed at 0.6 keV and fixed 1σ width of 50 eV gave an upper limit estimate for any oxygen emission line of 20 eV at the 90 per cent confidence level.

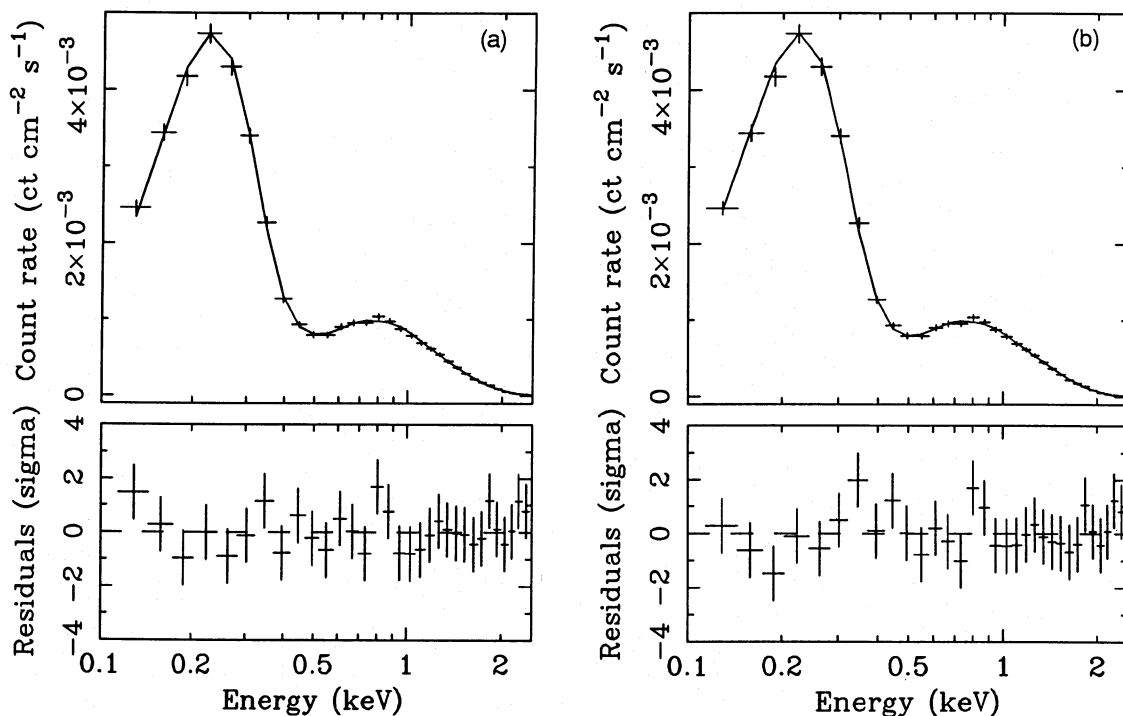


Figure 2. Counts spectra and residuals for Mrk 841. (a) Shows a power-law plus warm absorber model fit, which gives an acceptable χ^2 , as does (b) a power-law plus blackbody fit. We are unable to distinguish between these models with the resolution of the PSPC. However, these spectral fits and the observed variability both illustrate the multicomponent nature of the PSPC spectrum. Table 1 shows the details of the parameters.

Note that, in deriving this upper limit, we have assumed that the *only* spectral components contributing to the PSPC band are a power law and this emission line.

4 MULTIWAVEBAND SPECTRAL ANALYSIS

In an attempt to constrain the form of the XUV continuum in Mrk 841, we have used the SWP spectrum derived using the prescription given in Section 2.2, and performed a spectral

analysis on the joint SWP/PSPC data set. The results are summarized in Table 2.

Intriguingly, we find that power-law plus warm absorber model derived from the PSPC data alone extrapolates very well into the UV band, and an acceptable fit is obtained to the joint SWP/PSPC data set (Table 2, line 1). The quality and implications of this fit are further illustrated in Fig. 3(a). Most remarkably, such a model does not require that the peak of the continuum emission occur in the XUV band.

Table 2. Fits to the combined X-ray and UV data. Model C is the warm absorber, and model D the accretion disc model of Ross et al. (1992).

Model	A_1 10^{-3}	Γ_1	M_{bh}	L/L_{edd}	N_{H} (10^{20} cm^{-2})	$\log N_{\text{H}}^*$ (cm^{-2})	$\log U$	$\chi^2_{\nu}/\text{d.o.f.}$
C.	6.19	$2.35^{+0.02}_{-0.03}$	–	–	2.2 (F)	$21.68^{+0.19}_{-0.20}$	$0.01^{+0.21}_{-0.10}$	0.82/33
D.	5.23	$2.37^{+0.02}_{-0.02}$	$< 1.5 \times 10^7$	0.31 (*)	2.2 (F)	–	–	1.24/32

*Unconstrained within the limits of the grid.

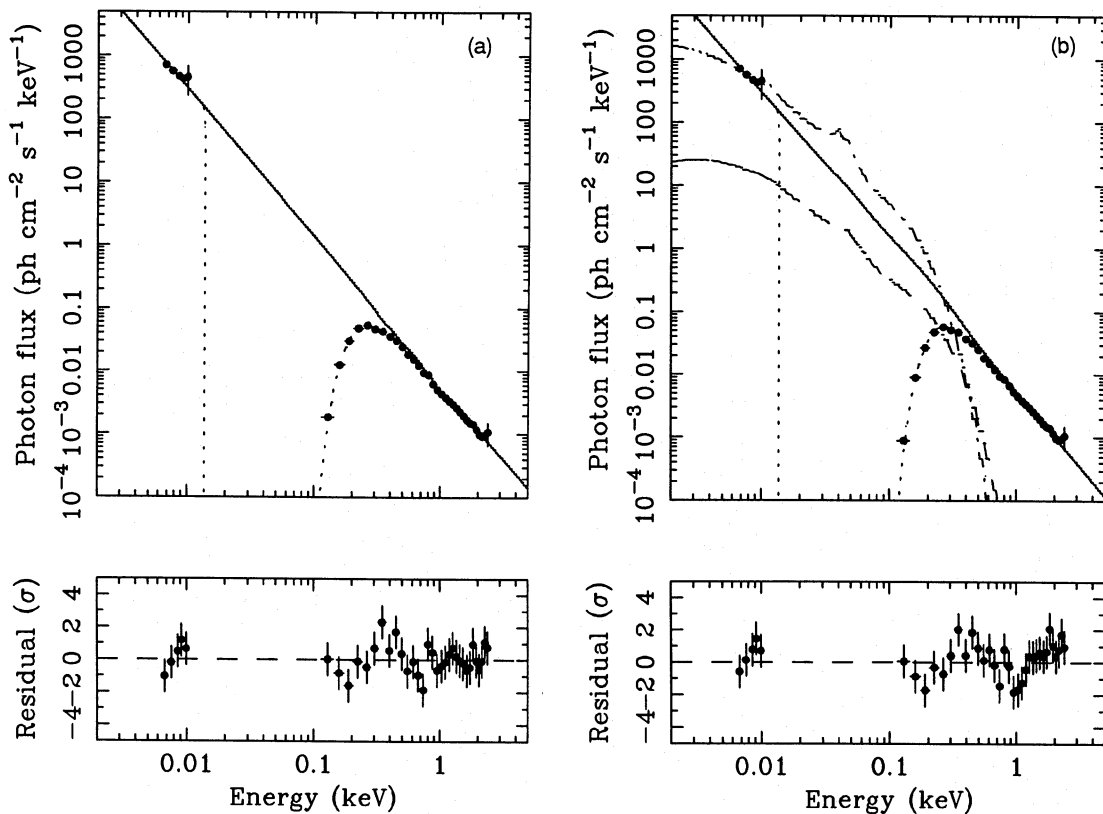


Figure 3. Deconvolved photon spectra and residuals for fits to the X-ray and UV data obtained for Mrk 841. Note that the X-ray data points derived from these fits are not unique and depend on the assumed model. (a) Shows the fit with a single power-law plus warm absorber, and illustrates the remarkable consistency of the UV data with the extrapolation of the best-fitting power-law in the PSPC band. The dotted line shows the spectrum after absorption by the Galactic column density; the solid line has the effects of absorption removed. The more complex disc fit with the model of Ross et al. (1992) is shown in (b). A power law was also included in this fit. The dotted line shows the best-fitting composite model (Table 2, line 2), and the solid line the same model ignoring absorption. The disc contribution to this fit is shown by the dashed line. Clearly the power-law component provides the bulk of the flux in both X-ray and UV bands, with the disc component (which has a very low black hole mass of $M_{\text{bh}} = 10^6 M_{\odot}$) contributing only to the lowest PSPC channels. To illustrate the problems with fitting a disc model with a higher black hole mass, the dot-dashed line shows the disc model with the best-fitting parameters of Ross et al. (1992) ($M_{\text{bh}} = 2 \times 10^7 M_{\odot}$, $L/L_{\text{edd}} = 0.28$), normalized to the UV data points. This disc spectrum is too steep to fit the soft excess in the *ROSAT* spectrum.

This is discussed further below. Nevertheless, we have attempted to fit the XUV emission from Mrk 841 with models representing a standard accretion disc spectrum.

As expected, the model described in Table 1 consisting of a power law plus (single temperature) blackbody, which gives a satisfactory fit to the PSPC data alone, is unable to provide a satisfactory fit to the joint SWP/PSPC data set. The blackbody temperature of ~ 75 eV derived from the X-ray data alone is too high to give a significant contribution at ~ 10 eV. However, as noted above, the blackbody fit is merely a simple parametrization of the putative ‘blue bump’ component. If this arises from an accretion disc, only the inner region of the disc would be expected to contribute to the soft X-ray emission, whilst the cooler, outer regions should provide the UV flux.

A large number of models have been presented in the literature to predict the spectrum emitted by the putative accretion discs in AGN (e.g. Shakura & Sunyaev 1973; Czerny & Elvis 1987; Sun & Malkan 1989). Even for the inner regions of standard α -discs, these models vary greatly in complexity from the simple multitemperature blackbodies (where each point in the disc is assumed to radiate at its effective blackbody temperature) to models including the effects of general relativity, realistic temperature/density structures through the disc, Comptonization in the outer layers or a corona etc.

Recently, Ross et al. (1992) have made new calculations of the emergent spectra from the inner, radiation-pressure-dominated regions of an α -disc which are fully self-consistent in the XUV regime. Furthermore, these workers apply their model to Mrk 841, and claim that archival UV and X-ray spectra are consistent with a face-on accretion disc (with $\alpha = 0.1$) surrounding a black hole of mass $2 \times 10^7 M_{\odot}$ emitting at 28 per cent of the Eddington luminosity. We have constructed a grid of these models and fitted them, in addition to a harder X-ray power law, to our joint SWP/PSPC spectrum of Mrk 841. Whilst our grid does not cover the full range of parameter space, it does encompass the best-fitting model found by Ross et al. (1992). In particular, we consider black hole masses $M_{\text{bh}} = 10^6 - 10^8 M_{\odot}$ and accretion rates $L/L_{\text{edd}} = 0.16 - 0.33$, and assume $\alpha = 0.1$, following Ross et al. However, we have allowed the normalization of the disc spectrum to be a free parameter, concentrating on the shape of the spectrum, rather than the luminosity. Whilst an acceptable fit was found with this model, examination of the spectrum revealed best-fitting parameters which indicated that the *power-law* component, rather than the model disc, contributes the bulk of the flux in the UV band. Fig. 3(b) illustrates this fit, which is detailed in Table 2. To understand this behaviour further we have shown an additional curve in Fig. 3(b), which represents the model with the best-fitting black hole mass and accretion rate of Ross et al. (1992) ($M_{\text{bh}} = 2 \times 10^7 M_{\odot}$ and $L/L_{\text{edd}} = 0.28$), normalized to our UV data. The spectrum in the PSPC band is clearly too soft to simulate the blackbody fit of Table 1.

A number of other (more simplistic) accretion disc models were also tried, including blackbody and modified blackbody forms. In none of the resulting fits did the disc spectrum contribute significantly to the UV and soft X-ray emission. These fits strongly imply that the XUV continuum in this object is better fitted by a power-law form than a thermal accretion disc spectrum, at least of the type which has been

considered so far. However, the spectrum almost certainly flattens from the $\Gamma = 2.4$ derived here, in the longer wavelength UV and optical. Indeed, formally we find an SWP spectral index of $\Gamma = 1.7 \pm 0.4$. This is consistent with the UV index quoted by Zheng & Malkan (1993) for this source, $\Gamma = 2.1$. These workers also found a slight flattening to $\Gamma = 1.9$ in the optical. We cannot therefore assume that the same power law that fits the XUV data described here extrapolates to lower frequencies. We conclude that the spectrum turns over somewhere in the optical/long-wavelength UV, but without simultaneous coverage in these bands we are unable to determine where. We now discuss possible models for the XUV continuum in Mrk 841 and their implications for the power source in AGN.

5 DISCUSSION

We have shown that Mrk 841 has a complex and variable spectrum in the soft X-ray band. The distinctive variability in the soft and hard bands indicates multiple components in the PSPC spectrum, but fits to the spectrum were unable to distinguish between two emission components, or a single power law modified by highly ionized gas in the line of sight. Either could produce the spectral variability we observe. Our most striking result emerges when we try to consider the UV data in relation to the X-ray spectrum. Specifically, the shape of the XUV continuum spectrum from 6 eV to 2 keV is entirely consistent with a single power law, albeit with minor modifications by the warm absorber in the PSPC band. Thermal accretion disc spectra of varying complexity were also tested against our data, but these were unable to produce a satisfactory fit. The reason for this appears to be that if the disc spectrum contributes substantially to the UV flux, the soft X-ray spectrum is too steep (soft) to fit the PSPC data. Before discussing the significance of our findings, we review the XUV continuum data in relation to those obtained at higher X-ray energies.

5.1 Consistency with previous hard X-ray data

We note that the best-fitting (photon) index from all the fits given in Table 1 ($\Gamma \sim 2.1 - 2.4$) is steeper than those obtained with *EXOSAT* and *Ginga* in the 2–10 keV band (G93). Such a spectral steepening in the *ROSAT* band is commonly observed in Seyfert galaxies (e.g. Turner, George & Mushotzky 1993). It is currently unclear whether the steepening arises as a result of additional soft emission or as an artefact of complex absorption. Pounds et al. (1994) have recently reported the results of simultaneous *Ginga* and *ROSAT* observations of Mrk 841. These workers found best-fitting models similar to those found above. Specifically, Pounds et al. found that either power-law plus warm absorber or power-law plus blackbody models provided acceptable fits to the composite 0.1–20 keV spectra.

Fixing $N_{\text{H}} = N_{\text{H}}(\text{Gal})$ and fitting the three *Ginga* observations of this source with an appropriate model (in this case, the reflection model of George & Fabian 1991 – the preferred model of G93), we find a weighted mean for the intrinsic hard spectral index $\Gamma = 1.61 \pm 0.15$. This is much flatter than that found in our PSPC fits ($\Gamma = 2.39 \pm 0.05$). Allowing N_{H} to be a free parameter in the *Ginga* fits gives $\Gamma = 1.8 \pm 0.3$, compatible at the $\sim 2\sigma$ level with our PSPC

data. Fits to the *Ginga* data with Γ fixed at 2.4 were also tried. These provided adequate fits to the 1990 and 1991 observations. The 1989 *Ginga* data (observation C of G93) gave a very poor fit with $\chi^2_\nu = 1.72/24$ d.o.f. The main discrepancy in this case is at the Fe K α line, where the model predicts too much flux. With such a steep slope, we also need to invoke substantial absorption of the 1–2 keV X-rays (which can be modelled with a cold column density $\sim 10^{22}$ cm $^{-2}$ in the 1990 and 1991 observations). At first sight, this would seem to be at odds with the PSPC spectrum, which shows little evidence of cold absorption $> 10^{20}$ cm $^{-2}$ intrinsic to the source (and also the substantial UV flux). However, a plausible explanation for this would be that a substantial column of highly ionized gas exists in the line of sight (if the gas were sufficiently warm so that the low-Z species were completely ionized, but that oxygen and the other moderate-Z elements were partially recombined). In this case the absorber would be transparent to ~ 0.1 – 0.2 keV X-rays, where the PSPC measures the cold column density, yet absorbing substantially at the lowest *Ginga* energies. We note, however, that even when a warm absorber is accounted for in the PSPC fits, the spectrum is still steeper than the $\Gamma = 1.8$ implied by the hard X-ray data. We therefore conclude that the steep soft X-ray component found in our *ROSAT* observation does not extrapolate to energies much higher than 2 keV, and probably does not represent a simple extension of the ‘canonical’ 2–10 keV underlying power law of $\Gamma = 1.8$ – 2.0 (Nandra & Pounds 1994). Our PSPC data are consistent with this harder power-law component contributing little to the flux in this band. A two-power-law fit to the spectrum, with the hard index fixed at $\Gamma = 1.8$, shows a hard flux level typical of the observations reported by G92. However, the fluxes of the hard and soft components become equal at 2 keV, and we can conclude that the PSPC spectrum is dominated by an additional soft component. An interesting consequence of this is that the softer component carries the bulk of the power. Integration of the steep ($\Gamma = 2.4$) power law between our observed limits (60 eV to 3 keV) gives a soft luminosity of $L_s = 1.1 \times 10^{45}$ erg s $^{-1}$. The hard X-ray luminosity is less certain, but for the highest flux state observed by *Ginga* (roughly the highest flux allowed by our two-power-law fit) and a photon index of $\Gamma = 1.8$, the harder power law would have to extend to 100 MeV to have the same flux as the soft component. If we assume, more realistically, that the spectrum extends to about 500 keV, we obtain a hard luminosity $L_h = 3.4 \times 10^{44}$ erg s $^{-1}$, a factor 3 lower than the soft power.

5.2 Nature of the XUV continuum

What, then, is the nature of the XUV continuum? Our analysis has shown that the spectrum is described by a power law which becomes visible at around 2 keV, extending to the short-wavelength UV. The spectrum must then turn over in the long-wavelength UV and optical, to account for the flattening there. The power-law nature of the extreme ultraviolet emission implies that accretion disc models would need to be modified substantially to fit our data set.

In particular, if disc spectra are to account for substantial luminosity in both the UV and soft X-ray regimes, a process must exist which significantly hardens the disc spectrum in the PSPC band. An obvious candidate is Comptonization –

the highly ionized outer layers of the disc, or a corona above it could Compton scatter some of the disc photons, producing a quasi-power-law spectrum in the soft X-ray. We can estimate parameters for the scattering plasma based on the observed spectral shape. The Compton y parameter of the scattering corona (of temperature T , Thomson optical depth τ_T) when $\tau_T \leq 1$ is given by

$$y = \frac{4kT \max(\tau_T, \tau_T^2)}{m_e c^2} = \frac{4}{(\Gamma + 2)(\Gamma - 1)},$$

where m_e is the electron mass, and c is the speed of light. Our observed spectral index of $\Gamma = 2.4$ therefore gives $y = 0.65$. (A slightly lower value is obtained if we use the more accurate formulae of Zdziarski (1985).)

This Compton y parameter can then be due to a low temperature (few keV) and high optical depth [$\tau_T \sim$ few medium such as produced in high-compactness, non-thermal models of the primary spectrum (Zdziarski & Coppi 1991)]. Alternatively, it could be a corona with a high temperature (~ 100 keV) and lower optical depth ($\tau_T \sim 0.4$) such as that envisaged in models where the hard X-rays are produced by an electron population with a thermal distribution (e.g. Haardt & Maraschi 1991). There are problems with both models, since in the first, the iron K-line reflected from the disc would be smeared out by Compton scattering (a problem for all high-compactness, pair-cascade models for Seyfert 1 galaxies) and the second means that the $\Gamma = 2.4$ spectrum should be the primary X-ray power law. However, we have argued on the basis of the *Ginga* data that the primary hard X-ray spectrum has $\Gamma \sim 1.8$. A plausible solution is that there is a range of Compton y parameters in the corona. We require a range of $\Gamma = 1.8$ – 2.4 , so y should vary by a factor of ~ 2 , due to a range of τ_T and/or kT in the corona. Thus, in this model, the entire UV to γ -ray continuum of this AGN can be accounted for by essentially the same mechanism. We note that the energy input for the corona could be provided by localized magnetic loops in the disc, in which case some regions of the disc could undergo substantial local heating, further hardening the spectrum.

X-ray/UV variability data should clarify the nature and origin of the blue bump in active galaxies. In particular, if the XUV continuum is due to Comptonized disc emission, we expect the short-wavelength UV and X-rays to vary simultaneously. Changes can be driven either by variations in the seed spectrum (presumably the UV/optical disc continuum), or by fluctuations in the optical depth and/or temperature of the scattering corona. In the first case, we would expect to observe near-simultaneous variations in the optical/UV/X-ray, as the proportion of scattered photons remains constant. There should be no significant changes of spectral shape in the XUV region, as this is only weakly dependent on the shape of the seed photon distribution. However, if only the optical depth of the scatterer changes, more of the seed photons are scattered, which could give changes in the Comptonized far-UV and soft X-ray flux without corresponding variations in the optical. The spectral index of the XUV continuum should be anticorrelated with the flux, as the spectrum is hardened by multiple scatterings as τ_T increases. Finally, if the temperature of the corona changes, we expect variations primarily on the soft X-ray component, assuming that the spectrum ‘pivots’ in the UV. Again, the

XUV index should be anticorrelated with the soft X-ray flux, the spectrum hardening as the temperature increases.

In the case of the model in which the disc is heated locally by X-rays, we expect variations in the soft X-rays to be largely uncorrelated with those in the UV, as the UV comes from a more extended region of the disc. Changes in the reprocessed soft X-ray flux should be driven by variability of the hard power-law component, whereas those of the UV and optical may have longer time-scales, and arise from thermal or viscous instabilities.

As we have already noted, the very rapid variations in spectral shape found in our *ROSAT* observation could be explained by changes in the ionization parameter and/or column density of an ionized absorber. These variations show that, at least on short time-scales, the spectrum hardens as the flux *decreases*, and variations in the soft X-rays have greater amplitude than the hard band. Flux-correlated changes in the ionization parameter of the ionized gas would have just this effect. On the other hand, these variations cannot be explained by a single Comptonized component with changing temperature, which should produce greater variations at higher energies and in the opposite sense to that observed. For similar reasons, a variable optical depth is ruled out. Variations in the seed flux on these time-scales seem most unlikely. The above conclusions for the origin of the spectral variability do not hold if the soft X-ray spectrum is dominated by different emission components in the two chosen energy bands (0.1–0.4 and 1.0–2.5 keV). In this case, independent variability of the two components can account for the spectral changes. However, our spectral fits suggest that this is not the case and, on balance, it seems most likely that the short-time-scale spectral variability is, in fact, due to the warm absorber rather than an additional soft component. Further progress on the origin of the spectral changes could be made if simultaneous X-ray and UV variability data were available.

5.3 Conclusions

We have shown that Mrk 841 exhibits short-time-scale variations, accompanied by spectral variability in the soft X-ray band. The soft X-ray spectrum is consistent with a power law modified either by absorption in highly ionized gas, or additional soft emission. The extrapolation of the *ROSAT* power law connects to the UV spectrum observed by the *IUE* short-wavelength camera. Disc models for the blue bump in this source may require substantial Comptonization of the basic spectrum, with a power-law 'tail' pivoting in the UV. The derived temperature for the Comptonizing medium is similar to that suggested by thermal models of the harder X-rays, which suggests that the entire UV to γ -ray continuum may be produced by Comptonization of the disc spectrum by a corona with variable optical depth and/or temperature. Further simultaneous observations in the soft X-ray and ultraviolet of this source, and others like it, should

clarify the nature and origin of the continuum emission of active galaxies.

ACKNOWLEDGMENTS

We thank Richard Saxton for his work on *ASTERIX*, Randy Ross for use of his accretion disc model, Tahir Yaqoob for use of his warm absorber model, and Paul Barr for assistance converting the *IUE* data to XSPEC format. We acknowledge the financial support of the SERC (KN), Royal Society (ACF), and Universities Space Research Association (IMG, TJT).

REFERENCES

- Arnaud K. A. et al., 1985, *MNRAS*, 217, 105
 Clavel J. et al., 1991, *ApJ*, 366, 64
 Clavel J. et al., 1992, *ApJ*, 393, 113
 Czerny B., Elvis M., 1987, *ApJ*, 321, 305
 Elvis M., Lockman T. R., Wilkes B., 1989, *AJ*, 97, 777
 Fiore F., Elvis M., Mathur S., Wilkes B. J., McDowell J. C., 1993, *ApJ*, 415, 129
 George I. M., Fabian A. C., 1991, *MNRAS*, 249, 352
 George I. M., Nandra K., Fabian A. C., Turner T. J., Done C., Day C. S. R., 1993, *MNRAS*, 260, 111 (G93)
 Guilbert P. W., Rees M. J., 1988, *MNRAS*, 233, 475
 Haardt F., Maraschi L., 1991, *ApJ*, 380, L51
 Harris A. W., Sonneborn G., 1987, in Kondo Y., ed., *Exploring the Universe with the IUE Satellite*. Reidel, Dordrecht, p. 729
 Hasinger G., Turner T. J., George I. M., Boese G., 1992, *Legacy* No. 2
 Lightman A. P., White T. R., 1988, *ApJ*, 335, 57
 Malkan M. A., Sargent W. L. W., 1982, *ApJ*, 254, 22
 Morrison R., McCammon D., 1983, *ApJ*, 270, 119
 Nandra K., Pounds K. A., 1992, *Nat.*, 359, 215
 Nandra K., Pounds K. A., 1994, *MNRAS*, 268, 405
 Nandra K. et al., 1993, *MNRAS*, 260, 504
 Pfeiffermann E. et al., 1987, *Proc. SPIE*, 733, 519
 Pounds K. A., Nandra K., Fink H. H., Makino F., 1994, *MNRAS*, 267, 193
 Rees M. J., 1983, *ARA&A*, 22, 471
 Ross R. R., Fabian A. C., Mineshige S., 1992, *MNRAS*, 258, 189
 Shakura N. I., Sunyaev R. A., 1973, *A&A*, 24, 337
 Shields G. A., 1978, *Nat.*, 272, 706
 Sonneborn G., Oliverson N. A., Imhoff C. L., Pitts R. E., Holm A., 1987, *NASA IUE Newsletter*, 32
 Sun W.-H., Malkan M. A., 1989, *ApJ*, 346, 68
 Trümper J., 1983, *Adv. Space Res.*, 4, 241
 Turner T. J., Weaver K. A., Mushotzky R. F., Holt S. S., Madejski G. M., 1991, *ApJ*, 381, 85
 Turner T. J., George I. M., Mushotzky R. F., 1993, *ApJ*, 407, 566
 Turner T. J., Nandra K., George I. M., Fabian A. C., Pounds K. A., 1993, *ApJ*, 419, 217
 Yaqoob T., Warwick R. S., 1991, *MNRAS*, 248, 773
 Zdziarski A. A., 1985, *ApJ*, 289, 514
 Zdziarski A. A., Coppi P. S., 1991, *ApJ*, 376, 480
 Zheng W., Malkan M. A., 1993, *ApJ*, 415, 517